European Journal of Neuroscience, Vol. 25, pp. 2034–2044, 2007 doi:10.1111/j.1460-9568.2007.05425.x

Novel stimulus-induced calcium efflux in *Drosophila* mushroom bodies

Yueqing Peng[1,2] and Aike Guo[1,3]
[1]Institute of Neuroscience, Key Laboratory of Neurobiology, Shanghai Institutes for Biological Sciences, Chinese Academy of Sciences, 320 Yueyang Road, Shanghai 200031, China
[2]Graduate School of Chinese Academy of Sciences, Beijing 100049, China
[3]State Key Laboratory of Brain and Cognitive Science, Institute of Biophysics, Chinese Academy of Sciences, 15 Datun Road, Chaoyang Dist.,Beijing 100101, China

Keywords: calcium imaging, calcium signals, electrical stimulation, GABA receptor, sodium–calcium exchanger

Abstract

The mushroom body (MB) is an important part of the *Drosophila* brain, and is involved in many behaviors, including olfactory learning and memory and some visual cognition. However, the physiological properties of MB neurons remain elusive. Here we used a calcium-imaging technique to study calcium signals in *Drosophila* MB. We found that, rather than increasing calcium spread, electrical stimuli dramatically decreased calcium signals in the terminals of MB fibers. This novel calcium decrease occurred at all developmental stages from larvae to adults, but was specific for certain regions of the MB neurons. GABA receptor blockade promoted calcium propagation through the MB fibers, but did not disrupt the stimulus-induced decrease in calcium. Furthermore, this decrease in calcium was independent of extracellular calcium concentration and was not due to altered uptake by intracellular calcium stores and mitochondria. Rather, we found that inhibition of sodium–calcium exchangers significantly attenuated the stimulus-induced decrease in calcium, whereas the decrease persisted when membrane calcium pumps were blocked. Our findings indicate that MB neurons exhibit a novel stimulus-induced calcium efflux, which may be importantly regulated by sodium–calcium exchangers in the *Drosophila* MB.

Introduction

Calcium ions (Ca^{2+}) are essential intracellular messengers responsible for controlling numerous cellular processes (for reviews, see Berridge *et al*., 2000, 2003; Carafoli, 2002). Once Ca^{2+} has carried out its signaling functions, it is rapidly removed from the cytoplasm by various mechanisms (Berridge *et al*., 2003; Guerini *et al*., 2005). The plasma membrane Ca^{2+}-ATPase (PMCA) pump and the Na^{+}/Ca^{2+} exchanger (NCX) remove Ca^{2+} to the extracellular space whereas the sarco-endoplasmic reticulum ATPase (SERCA) pump returns Ca^{2+} to the internal stores. In addition, mitochondria also help regulate intracellular calcium levels (Bianchi *et al*., 2004; Saris & Carafoli, 2005).

Recent studies have shown a growing interest in elucidating the roles of the NCX (for reviews, see Blaustein & Lederer, 1999; Philipson & Nicoll, 2000; Annunziato *et al*., 2004). Based on its dependence on potassium ions, the NCX family can be divided into two categories: NCX exchangers and NCKX exchangers. *Drosophila* encodes three NCX genes. One is *Calx* (Ruknudin *et al*., 1997; Schwarz & Benzer, 1997), which is homologous to mammalian NCX exchangers. The other two are *Nckx30C* (Haug-Collet *et al*., 1999) and *Nckx-X* (Winkfein *et al*., 2004), which are NCKX exchangers. Although these three genes have been cloned and characterized on a molecular level, little is known about their physiological functions *in vivo*. Recent research has shown that the Na^{+}/Ca^{2+} exchanger CalX plays an essential role in light activation, adaptation and cell survival in photoreceptors (Wang *et al*., 2005). However, to date there have been no reports about the physiological roles of NCX in other brain regions in *Drosophila*.

In insects, the mushroom body (MB; for reviews, see Heisenberg, 1998, 2003; Strausfeld *et al*., 1998; Zars, 2000) is an important brain structure for olfactory learning and memory (Heisenberg *et al*., 1985; De Belle & Heisenberg, 1994; Connolly *et al*., 1996) and some visual cognitive behaviors, such as context generalization (Liu *et al*., 1999) and choice behavior (Tang & Guo, 2001). The MB comprises thousands of densely packed parallel neurons (2500 Kenyon cells), which receive both cholinergic and GABAergic inputs in the calyx (Yasuyama *et al*., 2002). Furthermore, the MB exhibits large-scale rearrangement during metamorphosis (Armstrong *et al*., 1998). Neurons projecting into the γ lobe are born first, prior to the mid-3rd instar larval stage, after which α′/β′ and α/β neurons are subsequently born (Lee *et al*., 1999).

Although much is known about the MB, knowledge of its physiological properties is quite lacking, due to the extreme difficulty of electrophysiological access to the tiny Kenyon cells. In the last decade, the development of calcium imaging using genetically encoded indicators has provided a powerful tool to investigate neuronal responses *in vivo* (Miyawaki *et al*., 1997, 1999; Nakai *et al*., 2001). By taking advantage of calcium-imaging techniques in *Drosophila*, here we have shown that electrical stimulus (ES) in the MB dramatically evoked a spreading calcium efflux. NCX probably

Correspondence: Dr A. Guo, [1]Institute of Neuroscience, as above.
E-mail: akguo@ion.ac.cn

Received 30 September 2006, revised 18 January 2007, accepted 22 January 2007

contributes to this ES-induced spreading calcium decrease. Our study provides a novel example of calcium decrease, which may be important for controlling neurotransmitter release in the neuronal terminals.

Materials and methods

Fly stocks

All fly stocks were cultured on standard *Drosophila* medium at room temperature (Guo *et al*., 1996). UAS-EGFP transgenic flies were crossed with 247-GAL4 to visualize the structure of the MBs. To monitor calcium activity, we crossed UAS-GCamp flies (3rd chromosome), which were kindly provided by Dr Yi Zhong (Cold Spring Harbor Laboratory, NY, USA), with either MB-specific GAL4 lines OK107-GAL4, 201Y-GAL4, C739-GAL4, 1471-GAL4 and H24-GAL4 or the control line GH146-GAL4. Progeny flies were used for all experiments.

Optical recording

Brains were dissected in normal insect saline (128 mM NaCl, 2 mM KCl, 35.5 mM sucrose, 4 mM $MgCl_2$, 1.8 mM $CaCl_2$, 5 mM Hepes, pH = 7.3–7.4, osmolarity = 290–300 mOsm) except for the calcium-free solution (1.8 mM $CaCl_2$ was replaced with 2 mM EGTA) and sodium-free solution (NaCl was replaced with molar equivalent LiCl or NMDG). The whole brain was mounted beneath a water immersion lens (Zeiss, 40×). Fluorescent images (about 256 × 256 pixels) were collected (1 frame per second) at room temperature by using a cooled CCD camera (Spot-RT, Diagnostic Instruments, USA) and a shutter/filter wheel (Lambda 10-2, Sutter Instruments, USA) controlled by MetaFluor software (Universal Imaging Corp., USA). The exposure time per frame was about 150 ms. The filters for excitation and emission light were at a bandwidth of 450–490 nm and long pass of 515 nm, respectively. A conventional fluorescence microscope (Zeiss) was used for all experiments of calcium imaging. To view the MB structure, 1-μm optical sections were acquired using a Zeiss LSM 510 META NLO upright two-photon microscope equipped with a water immersion lens (Zeiss, 40×). The light source was a titanium–sapphire (Ti:Sa) laser (Coherent, Mira 900-F) running at a wavelength of 900 nm. All optical slices of one brain were merged using Zeiss LSM 510 software.

Drug application and electrical stimulus

All drugs were purchased from Sigma. Thapsigargin and picrotoxin (PTX) were dissolved in DMSO (final concentration < 0.1%). The pH 9.0 solution was modified from normal saline with CsOH. Only fresh pH 9.0 solution was used for the experiments. Drugs were applied to the brain tissue with bath superfusion (ALA-VM8, ALA Scientific Instruments) or bath incubation. Thapsigargin was applied 3–5 min before the electrical stimulus, and the brain tissues were incubated in ruthenium red solution for 20–30 min before stimulation. Extracellular electrical stimulus was applied for 500 ms through patch pipettes (1–3 MΩ) filled with normal saline. The stimulus location was near the heel of the MB lobes, which was found under background fluorescence of the GCamp. The criterion determining the intensity of the electrical stimulus was determined by those stimuli inducing significant calcium responses in the MB lobes. After testing several different intensities, we found that a 200-μA current with a 200-ms duration at 20 Hz was most suitable for inducing explicit responses in the MB (Iso-Flex; Master-8 Stimulator, AMPI, Jerusalem, Israel). Weak stimuli (50–100 μA) on occasion did not reliably induce significant calcium responses, whereas strong stimuli often damaged the tissue.

Data analysis

Images of calcium activity were false color-coded and presented as relative changes in fluorescence intensity normalized to baseline fluorescence ($\Delta F/F$). F was calculated for each pixel at the frame just prior to the electrical stimulus. The value ΔF was obtained for each pixel by subtracting the corresponding F from the fluorescence intensity at a certain frame. However, the $\Delta F/F$ values in the curves were the averages of fluorescence change within the region of interest. The time labels inside the figures are the relative time to the stimulus onset. ANOVAs and Student's *t*-tests (two-tailed *P*-value) were used for statistical analyses. *Post-hoc* Tukey's HSD tests were conducted to evaluate the differences between individual groups. Asterisks (*) indicate $P < 0.05$. The number of samples represents the number of different MBs. Error bars in the figures represent the SEMs.

Results

Electrical stimulus induced novel calcium decrease in the MB

By using the UAS/GAL4 system in *Drosophila*, the calcium indicator GCamp (Nakai *et al*., 2001; Wang *et al*., 2004) was expressed in the MB, driven by MB-specific GAL4 lines. We reconstructed the MB structure to view the compartments and subcompartments through two-photon microscopy (see above). As shown in Fig. 1A, the MB structure consists of the calyx, peduncle and lobes (vertical lobes: α/α′; medial lobes: γ/β/β′). For morphological observation, we chose the 247 line, which is an MB-specific GAL4 line with little leaky expression. However, to visualize better the calcium activity in subsequent calcium-imaging experiments, we used the OK107 line as the MB expression driver, due to its strong expression. Note that the calcium-imaging experiments were done with a conventional fluorescence microscope. Therefore, the resolution limited our ability to distinguish the MB subcompartments.

To observe the calcium signals, we directly applied an ES near the heel of the MB lobes (Fig. 1B). We found, surprisingly, that the fluorescence decreased to below baseline in the distal part of the ipsilateral medial lobes (γ/β/β′) after stimulation (Fig. 2A and B). Meanwhile, the electrical stimulus did not have any effect on the contralateral MB lobes. Approximately 60 s after stimulation, the calcium concentration, which was positively correlated with the fluorescence intensity, dropped to the minimum level noted. Serial images of relative calcium change showed that the regions of the observed calcium decrease covered a large portion of the ipsilateral medial lobes but not the stimulus site (Fig. 2C). Meanwhile, the calcium increase observed at the stimulus site did not propagate through the MB fibers. According to previous studies, most neuronal activity is conducted by the increase in calcium after electrical stimulation. We therefore described this ES-induced calcium decrease in the non-stimulus region as a spreading calcium decrease.

To test whether the intensity of the ES was sufficient for neuronal activation and calcium propagation, we applied currents of varying intensities to stimulate the MB. Within a certain range (50–200 μA), the stronger currents induced higher amplitudes of spreading calcium decrease (Fig. 2D). At a certain level of stimulation (200–400 μA), the amplitude reached a plateau. Data analysis revealed that the magnitude of the calcium decrease was negatively correlated with the degree of calcium influx at the stimulus site (Fig. 2E). This correlation suggests

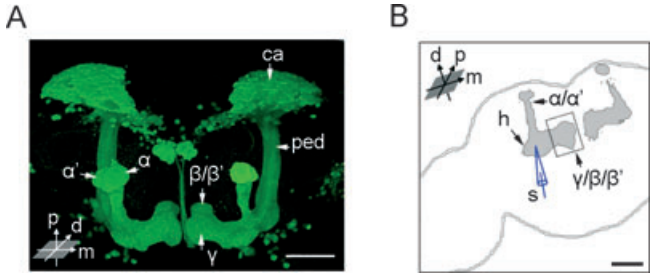

FIG. 1. The structure of the MB and a schematic of stimulus site. (A) The calcium indicator GCamp was expressed in the MB, driven by the 247 GAL4 line. The MB structure was reconstructed by superimposition of optical sections through two-photon microscopy, which includes the calyx (c), peduncle (ped), and lobes (vertical lobes: α and α′; medial lobes: γ, β and β′). Note that all single somata and the medial cluster do not represent MB neurons, but may be labeled by leaky expression of the GAL4 line. (B) The schematic shows the site of electrical stimulus (s), which is near the heel (h) of the MB lobes. The distal portion of the medial lobes (γ/β/β′) is the main region of interest (the boxed area). The contour outside the MB represents the outline of the *Drosophila* brain. Brain coordinates are shown in the corners. The gray surface in the coordinates is always vertical to the surface of images in this figure and all subsequent figures. (Abbreviations: p, posterior; d, dorsal; m, medial). The scale bars represent 50 μm.

that stronger activation in one region of the MB induced a great spreading calcium decrease in another region.

The MB primarily comprises tripartite subunits, α/β neurons, α′/β′ neurons and γ neurons (Crittenden *et al*., 1998). To evaluate the detailed properties of the MB neurons with a conventional microscope, different Gal4 lines were crossed with UAS-GCamp flies. We found that the ES-induced spreading calcium decrease was also observed in the medial lobes of the 201Y line (mainly the γ-lobe, a small part of the α/β-lobe; Fig. 3A). However, the same stimulation failed to evoke a significant spreading calcium decrease in either the medial or the vertical lobes of the C739 line (α/β-lobe-specific MB GAL4; Fig. 3B and C). These data suggest that the ES-induced spreading calcium decrease may be specific to the γ-lobe, but not the α/β-lobe of the MB, which was confirmed by studies in two other γ-lobe-specific GAL4 lines (1471 and H24). When compared with the C739 line, both the 1471 and H24 lines showed higher magnitudes of ES-induced spreading calcium decrease, although they exhibited a lower degree of calcium influx at the stimulus sites (Fig. 3C).

In *Drosophila* motorneuron terminals electrically stimulated with a train of action potentials, GCamp revealed increased fluorescence, and then a prolonged undershoot lasting seconds to minutes (Reiff *et al*., 2005). This undershoot has been interpreted to indicate increased bleaching of the fluorophore in the more fluorescent state. To exclude the possibility that the ES-induced fluorescence decrease in the MB

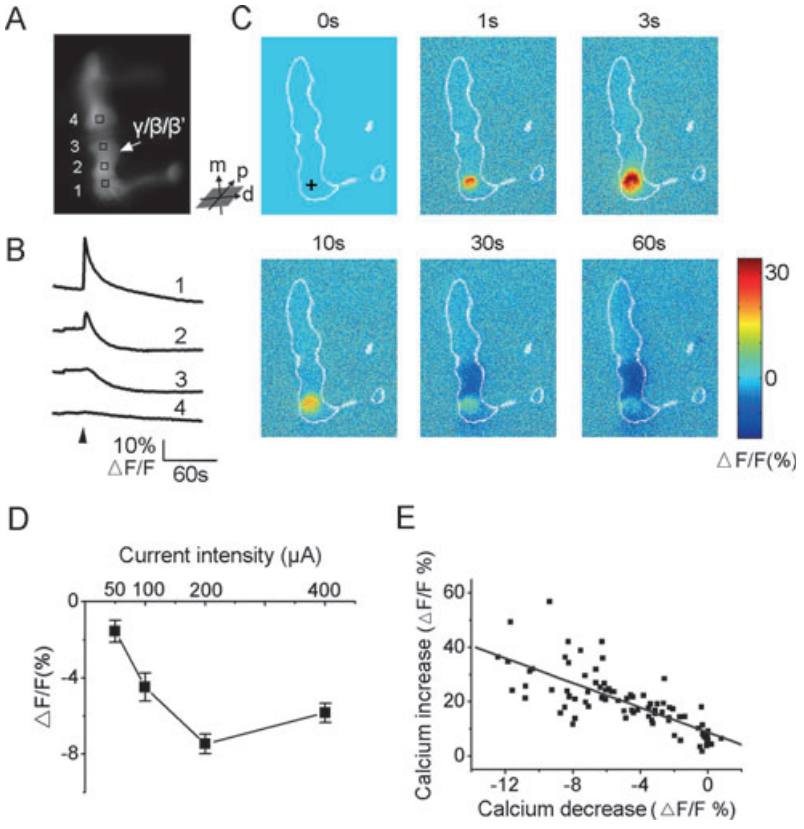

FIG. 2. Electrical stimulus-induced spreading calcium decrease in the terminals of the MB lobes. (A) GCamp expression revealed the background fluorescence of the MB, driven by the OK107-GAL4 line. Regions of interest are marked with small boxes. MB medial lobes (γ/β/β′) are marked with an arrow. Brain coordinates: p, posterior; d, dorsal; m, medial. (B) The curves of fluorescence change showed ES-induced calcium responses in the MB lobes, corresponding to the regions of interest in A. The stimulus onset is indicated by the arrowhead. (C) False colored series images illustrating the regions of relative calcium change in the MB lobes. The stimulus site is labeled with the cross. The times at the top refer to relative times after stimulation. The white outlines show the contours of the MB. (D) The curve of different stimulus intensities and the mean amplitudes of spreading calcium decrease in the MB terminals (region 3, $n = 87$). (E) The amplitudes of the spreading calcium decrease in region 3 correlated with the amplitudes of calcium influx in region 1, plotting all data from different stimuli. The straight line shows the linear regression of the data points ($R = –0.75$).

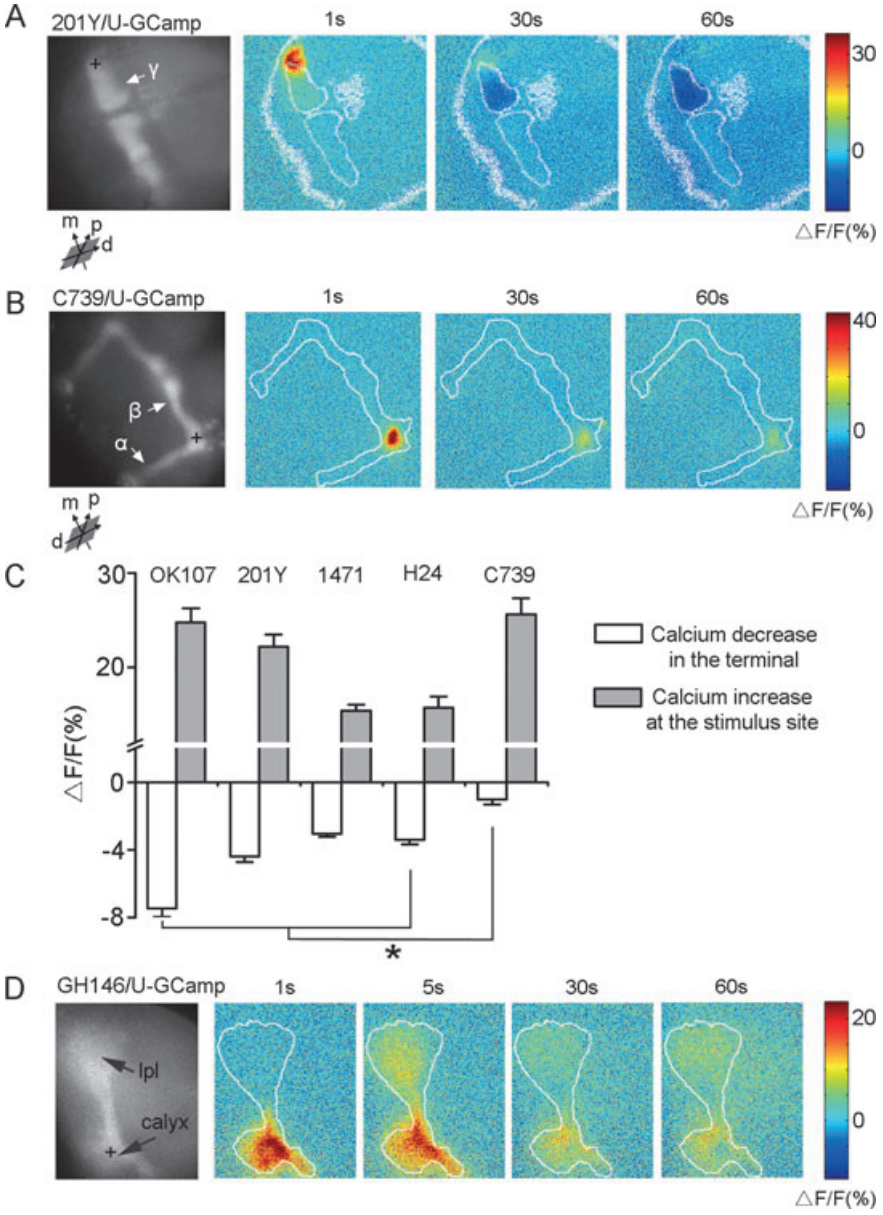

FIG. 3. The ES-induced spreading calcium decrease was largely specific to the MB γ-lobe. (A) False colored series images of ES-induced spreading calcium decrease in individual 201Y-GAL4/UAS-GCamp fly. The MB γ-lobe is indicated by the arrow. (B) False colored series images of calcium activity in individual C739-GAL4/UAS-GCamp fly. The α-lobe and β-lobe are indicated by the arrows. (C) Statistical analyses of the ES-induced spreading calcium decrease in the terminals of MB medial lobes and calcium influx at the stimulus sites in different MB GAL4 lines ($n = 25$, $n = 38$, $n = 46$, $n = 37$ and $n = 24$, respectively). The amplitude in the C739 line was significantly smaller than those in the other lines (ANOVA test, $P < 0.01$). (D) Electrical stimulus-induced calcium propagation through the projection neurons; no spreading calcium decrease occurred in GH146/UAS-GCamp flies. The MB calyx and lateral protocerebral lobe (lpl) are marked with the arrow. In A, B and D, the stimulus site is labeled with the cross. Brain coordinates: p, posterior; d, dorsal; m, medial.

lobe is due to photobleaching of GCamp, we also examined ES-induced calcium activity in projection neurons by using the GH146-GAL4 line. We found that there was no spreading calcium decrease in the projection neurons, and the calcium signal was propagated to the terminal of the fibers (Fig. 3D). This result suggests that the ES-induced spreading calcium decrease might be a physiological property specific to the MB lobes.

GABA-mediated Inhibition of calcium propagation in the MB

The ES-induced spreading calcium decrease was also recorded in the ipsilateral calyx (Fig. 4A). This finding suggests that the entirety of ipsilateral MB neurons may be inhibited after stimulation. Due to the presence of GABA receptors expressed in the MB calyx, we applied PTX (100 μM; an antagonist of $GABA_A$ receptors) and CGP54626 (50 μM; an antagonist of $GABA_B$ receptors; Wilson & Laurent, 2005) to explore the function of GABA inhibition in the ES-induced spreading calcium decrease.

In contrast to the highly localized calcium increases observed in the absence of PTX, we found that the ES-induced calcium increase at the stimulus site was propagated in the ipsilateral MB when $GABA_A$ receptors were blocked (Fig. 4B). However, following an initial rising phase, the calcium concentration in the MB terminal subsequently decreased. The amplitude of the ES-induced calcium decrease was not

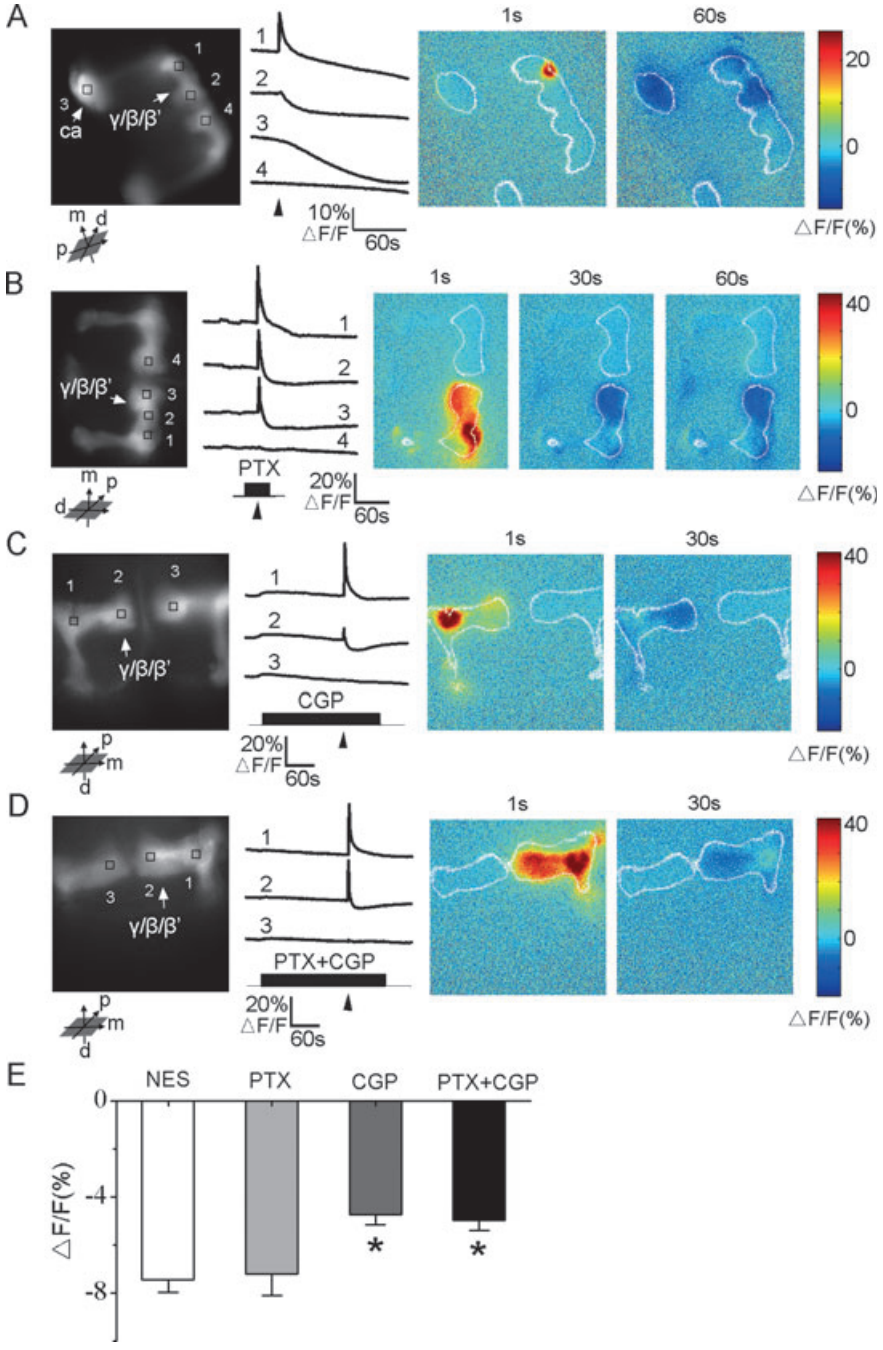

FIG. 4. GABA receptor inhibition influenced calcium propagation, but did not contribute to the ES-induced spreading calcium decrease in the MB. (A) Stimulation in the MB lobes (region 1) also induced a decrease in calcium in the ipsilateral MB calyx (c., region 3). (B) Inhibition of $GABA_A$ receptors with picrotoxin (PTX, 100 μM) promoted the ES-induced calcium propagation through the MB fibers, but did not eliminate the ES-induced calcium decrease. Drug application is indicated with the black bar. (C) Electrical stimulus induced a significant calcium decrease in the MB lobes after inhibition of $GABA_B$ receptor with CGP54626 ('CGP', 50 μM). (D) Effects of inhibition of both $GABA_A$ and $GABA_B$ receptors. (E) Statistical analyses of the amplitudes of the calcium decrease with the inhibition of GABA receptors ($n = 22$, $n = 25$, $n = 20$ and $n = 19$, respectively). Normal extracellular saline (NES) served as the control. In A–D, the stimulus site is region 1. MB medial lobes (γ/β/β′) are indicated with the arrows. Brain coordinates: p, posterior; d, dorsal; m, medial.

significantly different from the control (Fig. 4E). In addition, following perfusion with CGP54626, electrical stimulation still resulted in a significant calcium decrease in the MB medial lobes, although the amplitude was slightly diminished compared with the control (Fig. 4C and E). Furthermore, simultaneous application of both PTX and CGP54626 failed to block the ES-induced calcium decrease, although this dual application promoted calcium propagation through the MB fibers (Fig. 4D and E). Taken together, these data suggest that GABA neurotransmission, particularly through $GABA_A$ receptors, is responsible for limiting the spread of calcium increases in the MB, but is not responsible for the ES-induced spreading calcium decrease.

Pharmacological analysis of ES-induced calcium decrease

Intracellular calcium concentration can be decreased in two different ways. One is through uptake by calcium stores or mitochondria. The

other is through calcium efflux to the extracellular region. To examine whether the first possibility was responsible for the ES-induced spreading calcium decrease in the MB, we used thapsigargin (Tg, 5 μM), an inhibitor of the endoplasmic reticulum Ca^{2+}-ATPase, and ruthenium red (RR, 20 μM), an inhibitor of mitochondria calcium uniporter (Moore, 1971; Reed & Bygrave, 1974) to block calcium uptake by calcium stores and mitochondria, respectively. We found that the ES-induced spreading calcium decrease remained in the MB in both treatment conditions (Fig. 5A and B). Following RR treatment, the amplitude of the ES-induced calcium decrease was smaller than

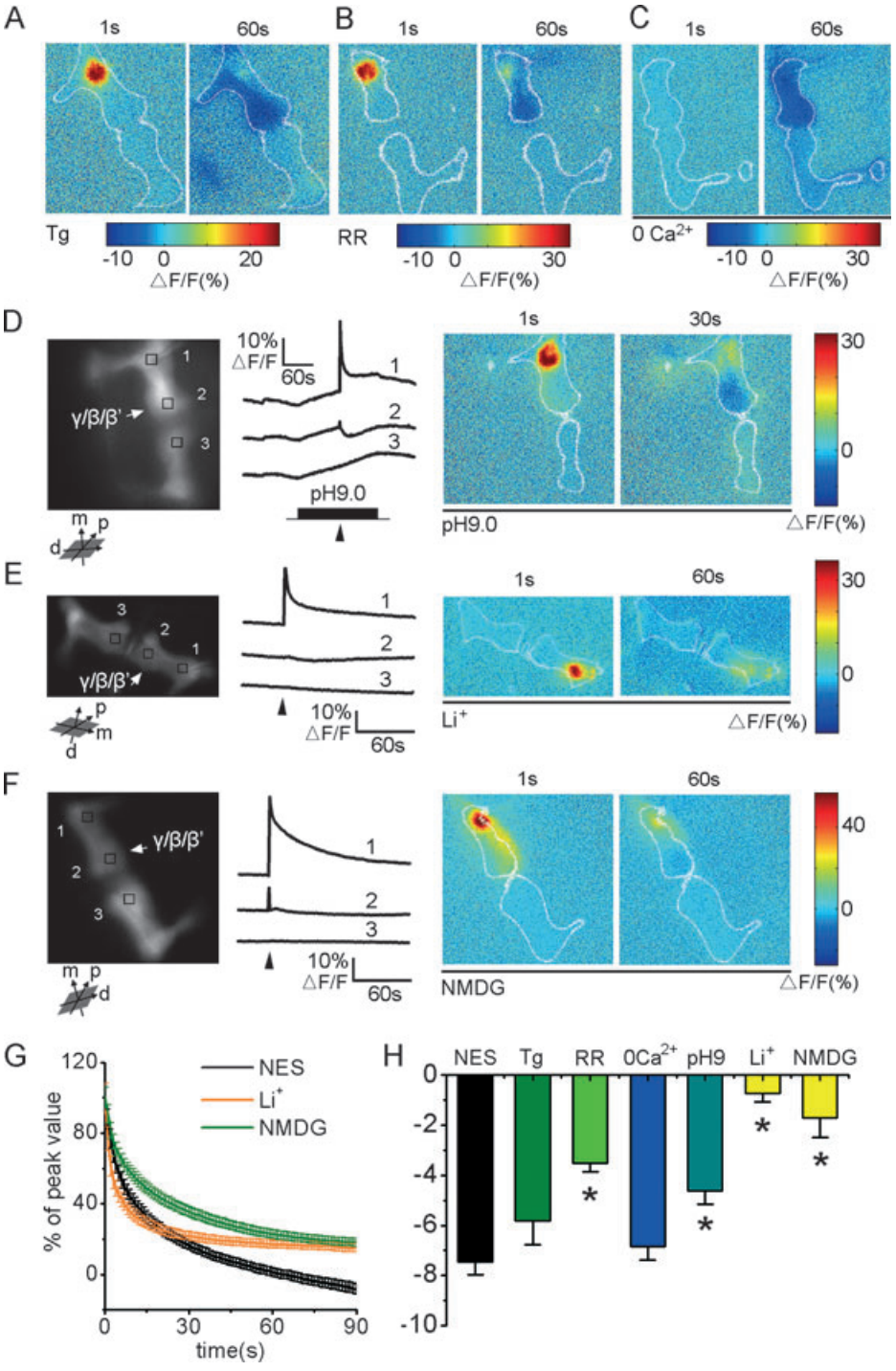

FIG. 5. Calcium clearance pharmacology. (A) Inhibition of intercellular calcium stores with thapsigargin (Tg, 5 μM) had no effect on the ES-induced spreading calcium decrease. (B) Effect of ruthenium red (RR, 20 μM) on ES-induced calcium decrease. (C) Effect of calcium-free solution. (D) Effect of pH 9.0 treatment, inhibiting the calcium pump (PMCA). (E) Inhibition of NCX with Li^+ eliminated the ES-induced spreading calcium decrease in the MB terminal. (F) Effect of NMDG on the ES-induced spreading calcium decrease. (G) Calcium decay kinetics at the stimulus site. Percentage decrease from the peak of calcium influx changed for 90 s in normal saline and sodium-free solutions ($n = 25$ for NES; $n = 21$ for Li^+ $n = 19$ for NMDG). (H) Statistical analysis of the amplitudes of ES-induced spreading calcium efflux in the various treatment conditions ($n = 25$, $n = 10$, $n = 33$, $n = 16$, $n = 17$, $n = 21$ and $n = 19$, respectively). Normal extracellular saline (NES) served as the control. Region 1 was the stimulus site for all cases. MB medial lobes (γ/β/β′) are marked with the arrows. Brain coordinates: p, posterior; d, dorsal; m, medial.

the control (Fig. 5H), which may have resulted from very weak background fluorescence in the RR solution (see Discussion). Although the incubation of the tissues with calcium-free saline prevented the calcium increase ordinarily induced by electrical stimulation, the spreading calcium decrease was unaffected (Fig. 5C and H). This suggests that the ES-induced calcium increase requires calcium entry through plasma membrane channels and that the ES-induced spreading calcium decrease requires neither extracellular calcium nor intracellular calcium stores. Based on these results, the first possibility was excluded and ES-induced spreading calcium decrease in the MB was probably caused by calcium efflux.

Normally neurons have two primary paths for calcium efflux: PMCA pumps and NCX. PMCA can be inhibited at high pH (Benham *et al*., 1992; Park *et al*., 1996). We found that the ES-induced spreading calcium decrease remained in a pH 9.0 solution (Fig. 5D). The amplitude of the spreading calcium decrease in this case was smaller than in the control (Fig. 5H), which might have resulted from the influence of high pH value on the baseline fluorescence of GCamp (Fig. 5D). NCX can be inhibited by replacement of sodium ions with lithium ions or *N*-methyl-D-glucamine (NMDG) (Fierro *et al*., 1998; Wanaverbecq *et al*., 2003). We found that the ES-induced spreading calcium decrease was eliminated following treatment with either lithium or NMDG saline (Fig. 5E and F). Calcium decay kinetics at the stimulus site showed the recovery of calcium concentration to the basal level was significantly slower in both sodium-free cases than that in normal saline (Fig. 5G). Statistical analyses indicated that the amplitudes of the spreading calcium decrease in both sodium-free salines were significantly different from those in normal saline (Fig. 5H). Together, these results indicate that NCX, and not PMCA, mediated the ES-induced spreading calcium decrease in the MB lobes.

To study further the function of NCX, we studied $Calx^A$ mutant flies (Wang *et al*., 2005), and KB-R7943, a selective inhibitor of reverse NCX (Iwamoto *et al*., 1996; Watano *et al*., 1996; Isaac *et al*., 2002). In both cases, we found that the electrical stimulus still induced a significant spreading calcium decrease in the distal part of the MB medial lobes, although the amplitudes of the spreading calcium decrease were slightly smaller than those in the control (see Supplementary material, Fig. S1). However, manipulation of the transmembrane Ca^{2+} and K^+ gradients could eliminate the ES-induced calcium decrease in the MB lobes (supplementary Fig. S1). This finding implies that the potassium-dependent exchanger (NCKX) may be importantly involved in the spreading calcium efflux (see Discussion).

Developmental effects on ES-induced calcium efflux

Because the MB exhibits a developmental metamorphosis, the physiological properties of the MB, including the regulation of calcium signals, might be different among the various developmental stages. To explore the developmental effects on ES-induced calcium efflux in the MB, we performed similar observations both in the 3rd instar larvae and pupae. We observed an ES-evoked spreading calcium decrease at both stages (Fig. 6A and B). Furthermore, the amplitudes of the spreading calcium decrease declined gradually during the developmental stages from larvae to adult (Fig. 6C). Further analysis indicated that the same electrical stimulus resulted in a larger calcium influx at the stimulus site in larvae than in adults. The amplitudes of the calcium influx and spreading calcium efflux in pupae were widely distributed. Data plotting of all developmental stages revealed a strong correlation between the amplitude of calcium influx at the stimulus site and the amplitude of the spreading calcium decrease in the MB terminal (Fig. 6D). Therefore, a larger spreading calcium efflux in early developmental stages might result from a larger calcium influx induced at the stimulus site. The observation of stronger ES-induced spreading calcium efflux in the 3rd instar larvae, in which stage γ neurons, but not α/β neurons, are born, supports the notion that this spreading calcium efflux is γ-lobe specific.

Non-electrical stimulus induced calcium efflux in the MB

To mimic physiological conditions, we also evaluated other types of stimuli in the MB. First, we applied 60 mM K^+ to the MB. High K^+ strongly depolarized MB neurons, which was shown as an initial increase phase of calcium signals (Fig. 7A). However, following the peak, there was a significant undershoot of calcium concentration in the MB lobes. This late phase of decreased calcium to below baseline levels was similar to the ES-induced spreading calcium efflux.

Second, we applied nicotine (10 μM) to the MB, as acetylcholine receptors are expressed in the calyx. We also found a similar undershoot of calcium signal following an increase phase in the MB lobes after application of nicotine (Fig. 7B). However, the undershoot was not significant in the calyx of the MB, where a strong calcium influx was observed. This finding suggests that there are different mechanisms of calcium clearance in the various MB compartments.

Taken together, non-electrical stimuli also induced a similar calcium efflux to below baseline levels in the MB lobes, which confirmed our reasoning that the MB has strong calcium exclusion in the lobes after neuronal activation.

Discussion

Although the MB is an essential brain structure for many behaviors in *Drosophila*, there are few available physiological studies because of the difficulty of electrophysiological recording *in vivo*. Here we used calcium imaging to study the activities of calcium signals in the MB. Our results support the conclusion that cytoplasmic calcium is directly removed by the Na^+/Ca^{2+} exchanger when the MB is activated. The spreading calcium efflux occurred at developmental stages from larvae to adults, but was primarily localized to the MB γ-lobe. Strong calcium clearance in the MB lobes was confirmed when the MB neurons were activated by high K^+ or nicotine. Our finding of a stimulus-induced calcium decrease is consistent with the previous observation that high K^+ induces a calcium undershoot in the MB lobes expressing camgaroo reporters (Yu *et al*., 2003).

Calcium imaging has been widely used in both vertebrates and invertebrates, particularly to study the olfactory system (Joerges *et al*., 1997; Fiala *et al*., 2002; Wang *et al*., 2003, 2004; Wachowiak *et al*., 2004). Unlike the normal odorant-elicited calcium increase, some olfactory receptor neurons respond to odorants with calcium decreases, which have been described in catfish (Restrepo & Boyle, 1991), humans (Rawson *et al*., 1997), salamanders (Delay & Dionne, 2002) and domestic cats (Gomez *et al*., 2005). Although the cellular signaling mechanism for such odorant-elicited calcium decreases has not yet been elucidated, these previous studies suggest that calcium decreases, as well as calcium increases, can act as a physiological signal. Therefore, in addition to the passive role of returning calcium concentrations to baseline levels following intracellular calcium increases, calcium decreases may also have active biological significance.

MB neurons express GABA receptors in the calyx. In crickets, GABA can induce a sustained calcium decrease in cultured MB neurons (Cayre *et al*., 1999). We also found that GABA application could induce a similar phenomenon in the *Drosophila* MB calyx (data

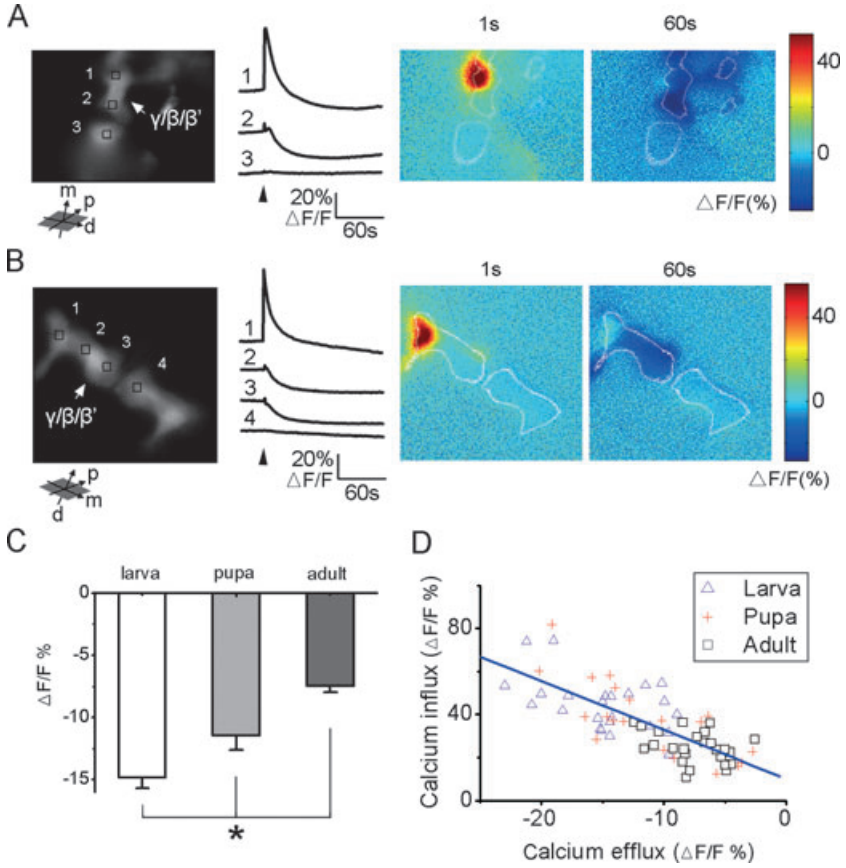

FIG. 6. ES-induced spreading calcium decrease appeared at the early developmental stages. (A) In the 3rd instar larvae, the electrical stimulus induced spreading calcium decrease in the ipsilateral MB lobes. (B) ES-induced spreading calcium decrease was also observed in pupae. (C) Statistical analysis illustrated that the amplitudes of calcium decrease dropped gradually during the developmental stages ($n = 24$, $n = 21$ and $n = 25$, respectively; ANOVA test, $P < 0.05$). (D) A correlation analysis revealed that the same stimulus intensity induced a larger calcium influx in larvae (open triangles) and pupae (crosses) than in adults (open boxes) (in total $n = 70$; $R = -0.75$). In A and B, the stimulus site is region 1. MB medial lobes (γ/β/β′) are indicated by the arrows. Brain coordinates: p, posterior; d, dorsal; m, medial.

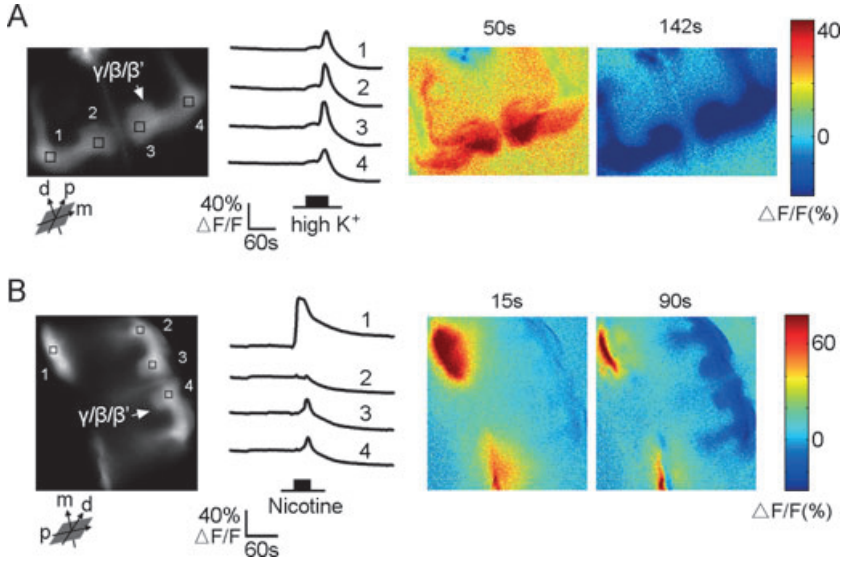

FIG. 7. Non-electrical stimulus induced calcium decrease in the MB lobes. (A) High K^+ (60 mM) caused large calcium undershoots in the MB lobes following an initial phase of increased calcium. (B) Nicotine (10 μM) strongly induced a calcium increase in both the calyx and lobes. Subsequently, calcium decreased to below baseline levels in the MB lobes. The times at the top of the false colored images refer to relative times after stimulation. MB medial lobes (γ/β/β′) are indicated by the arrows. Brain coordinates: p, posterior; d, dorsal; m, medial.

not shown). However, the inhibition of GABA receptors did not block the observed calcium decrease in the terminals of the MB lobes, which indicated that GABAergic transmission did not probably mediate the ES-induced spreading calcium decrease. On the other hand, the inhibition of GABA receptors caused a propagation of a calcium increase throughout the MB fibers after stimulation, which was not observed in normal cases. Note that the electrical stimulus was applied to the MB lobes. One possibility is that the stimulation may also activate GABAergic neurons, inducing recurrent inhibition of MB neurons. The feedback circuit of GABAergic neurons to the MB has been morphologically described in honeybees (Bicker *et al*., 1985; Grunewald, 1999; Ganeshina & Menzel, 2001). A previous immunolabeling study implied that GABAergic neurons might connect the α-lobe to the calyx in the *Drosophila* MB (Yasuyama *et al*., 2002). Therefore, we propose that there might exist a GABA-mediated negative feedback circuit in the *Drosophila* MB.

The physiological functions of NCX in the central nervous system are virtually unknown. Mice with an Na^+/Ca^{2+} exchanger 2 deficiency exhibited enhanced performance in hippocampus-dependent learning and memory (Jeon *et al*., 2003). In *Drosophila*, mutations of the Na^+/Ca^{2+} exchanger *calx* have a profound effect on activity-dependent survival of photoreceptor cells (Wang *et al*., 2005). Moreover, a loss of CalX activity resulted in a transient response to light, a dramatic decrease in signal amplification and unusually rapid adaptation. In the present study, our pharmacological findings suggested that NCX plays an important role in the ES-induced spreading calcium efflux in the terminal of the MB lobes. Replacement of Na^+ in the bath with Li^+ or NMDG inhibited both the NCX and the NCKX exchangers. When we blocked the NCX exchangers, but not the NCKX exchangers, with KB-R7943 (Iwamoto *et al*., 2001; Czyż & Kiedrowski, 2002), or evaluated $calx^A$ mutant flies, the electrical stimulus still resulted in a spreading calcium efflux in the MB lobes. Our results demonstrate that calcium efflux occurred in the axon terminals of the MB, which is consistent with the NCKX exchanger distribution in the axon terminals in rat supraoptic magnocellular neurons (Kim *et al*., 2003). Together these data suggest that NCKX exchangers might be the primary mechanism underlying the ES-induced spreading calcium efflux in the MB lobes. NCKX exchangers couple the entry of four Na^+ ions with the exclusion of one Ca^{2+} and one K^+ ion. Theoretically, high extracellular Ca^{2+} or K^+ could affect the amplitude of the calcium decrease, as the energy for Ca^{2+} transport by NCKX depends on the transmembrane Na^+, K^+ and Ca^{2+} gradients. We found that a ten-fold increase in Ca^{2+} (20 mM) or K^+ (20 mM) in extracellular saline eliminates the ES-induced calcium decrease in the MB lobes (supplementary Fig. S1). However, high calcium may be deleterious to the tissue, and high potassium can increase neuronal excitability or even depolarize neurons. In our experiments, we tried to avoid these side-effects by only recording freshly dissected tissues for a short time (less than 1 h) and only recording the ES-induced calcium responses in the resting period without the spontaneous calcium activity. Therefore, our results imply that NCKX exchangers might be the molecular mechanism underlying the calcium efflux in the MB. However, due to the shortage of specific inhibitors of NCKX exchangers and genetic mutants, we cannot further confirm the function of NCKX exchangers in the present study.

Besides the NCX, there are three other major possible mechanisms of calcium exclusion. The first is uptake by intracellular calcium stores. The application of thapsigargin had no effect on the spreading calcium decrease, therefore excluding a role for endoplasmic reticulum calcium uptake. The second one is calcium exclusion by PMCA. Many drugs inhibit PMCA on the intracellular side, which was technically difficult in this study. Therefore, we simply used a high pH value to block PMCA. Although the amplitude of the calcium decrease was smaller in high pH solution than that in the control, the ES-induced spreading calcium decrease was clearly observed in the MB lobes. On the other hand, pH value influences the fluorescence of green fluorescent protein (GFP) or other related proteins. Here we found the baseline of the fluorescence was changed under high pH conditions (Fig. 5D). Therefore, high pH might subtly modify the amplitude of the calcium decrease, which might result in the observed differences from the control. The last possible mechanism is calcium uptake by the mitochondrion, which can be ruled out in this case by the finding that the ES-induced spreading calcium decrease remained even after incubation with ruthenium red. Although the amplitude of the spreading calcium decrease was smaller, it is most likely that the red colour of the solution with ruthenium red reduced the resolution of the images.

Finally, our findings also pose some new and intriguing questions. What is the trigger of the Na^+/Ca^{2+} exchanger? Following drug application, we excluded some neurotransmitters, such as glutamate, octopamine and dopamine (data not shown). Why is the Na^+/Ca^{2+} exchanger activated in the spreading region of the MB lobes? What is the physiological significance of this calcium decrease? It is possible that the ES-induced calcium decrease is secondary to an increase that is either below the temporal or spatial limit of resolution of our imaging system, or it may be a primary, inhibitory response. However, in both cases, low calcium concentration is the common final result after the stimulation. We found that the recovery of calcium levels to baseline was very slow, often more than 3 min (data not shown). One possible explanation of this low calcium level is mutual inhibition among MB neurons by controlling neurotransmitter release in the axon terminals. In other words, the electrical stimulus activated a small group of MB neurons, which subsequently inhibited the surrounding MB neurons by jointly down-regulating calcium levels. The ES-induced calcium decrease was broadly observed in the MB terminals. This property of mutual inhibition can possibly be used to explain the alternative choice of the signals in the conflict situation, such as decision-making in *Drosophila* (Tang & Guo, 2001). Supposing that different groups of MB neurons conduct different signals, a good way to send one particular signal downstream is to inhibit other signals. Another possible explanation is self-inhibition: low calcium levels following a strong stimulation may block the subsequent signal or inhibit spontaneous neuronal activity. This property of self-inhibition can also be used to explain the temporal integration of neuronal signals, which contributes to the roles of the MB in associative learning in *Drosophila*.

Supplementary material

The following supplementary material may be found on www.blackwell-synergy.com

Fig. S1. Effects of NCX on ES-induced spreading calcium decrease.

Acknowledgements

This work was supported by grants from the National Science Foundation of China (Grants 30270341, 30630028 and 30621004), the Multidisciplinary Research Program (Brain and Mind) of the Chinese Academy of Sciences, the National Basic Research Program of China (G2000077800 and 2006CB806600), and the Precedent Project of Important Intersectional Disciplines in the Knowledge Innovation Engineering of the Chinese Academy of Sciences (Grants KJCX1-09–03 and KSCX2-YW-R-28).

Abbreviations

ES, electrical stimulus; MB, mushroom body;; NCKX, potassium-dependent exchanger NCX, Na^+/Ca^{2+} exchanger; NMDG, *N*-methyl-D-glucamine; PMCA, plasma membrane Ca^{2+}-ATPase; PTX, picrotoxin; RR, ruthenium red; SERCA, sarco-endoplasmic reticulum ATPase; Tg, thapsigargin.

References

Annunziato, L., Pignataro, G. & Di Renzo, G.F. (2004) Pharmacology of brain Na^+/Ca^{2+} exchanger: from molecular biology to therapeutic perspectives. *Pharmacol. Rev.*, **56**, 633–654.

Armstrong, J.D., de Belle, J.S., Wang, Z. & Kaiser, K. (1998) Metamorphosis of the mushroom bodies; large-scale rearrangements of the neural substrates for associative learning and memory in *Drosophila*. *Learn. Mem.*, **5**, 102–114.

Benham, C.D., Evans, M.L. & McBain, C.J. (1992) Ca^{2+} efflux mechanisms following depolarization evoked calcium transients in cultured rat sensory neurons. *J. Physiol.*, **455**, 567–583.

Berridge, M.J., Bootman, M.D. & Roderick, H.L. (2003) Calcium signalling: dynamics, homeostasis and remodelling. *Nat. Rev. Mol. Cell Biol.*, **4**, 517–529.

Berridge, M.J., Lipp, P. & Bootman, M.D. (2000) The versatility and universality of calcium signaling. *Nat. Rev. Mol. Cell. Biol.*, **1**, 11–21.

Bianchi, K., Rimessi, A., Prandini, A., Szabadkai, G. & Rizzuto, R. (2004) Calcium and mitochondria. mechanisms and functions of a troubled relationship. *Biochim. Biophys. Acta*, **1742**, 119–131.

Bicker, G., Schafer, S. & Kingan, T.G. (1985) Mushroom body feedback interneurons in the honeybee show GABA-like immunoreactivity. *Brain Res.*, **360**, 394–397.

Blaustein, M.P. & Lederer, W.J. (1999) Sodium/calcium exchange: its physiological implications. *Physiol. Rev.*, **79**, 763–854.

Carafoli, E. (2002) Calcium signaling: a tale for all seasons. *Proc. Natl Acad. Sci. USA*, **99**, 1115–1122.

Cayre, M., Buckingham, S.D., Yagodin, S. & Sattelle, D.B. (1999) Cultured insect mushroom body neurons express functional receptors for acetylcholine, GABA, glutamate, octopamine, and dopamine. *J. Neurophysiol.*, **81**, 1–14.

Connolly, J.B., Roberts, L.J., Armstrong, J.D., Kaiser, K., Forte, M., Tully, T. & Kane, C.J. (1996) Associative learning disrupted by impaired Gs signaling in *Drosophila* mushroom bodies. *Science*, **274**, 2104–2107.

Crittenden, J.R., Skoulakis, E.M., Han, K.A., Kalderon, D. & Davis, R.L. (1998) Tripartite mushroom body architecture revealed by antigenic markers. *Learn. Mem.*, **5**, 38–51.

Czyż, A. & Kiedrowski, L. (2002) In depolarized and glucose-deprived neurons, Na^+ influx reverses plasmalemmal K^+-dependent and K^+-independent Na^+/Ca^{2+} exchangers and contributes to NMDA excitotoxicity. *J. Neurochem.*, **83**, 1321–1328.

De Belle, J.S. & Heisenberg, M. (1994) Associative odor learning in *Drosophila* abolished by chemical ablation of mushroom bodies. *Science*, **263**, 692–695.

Delay, R.J. & Dionne, V.E. (2002) Two second messengers mediate amino acid responses in olfactory sensory neurons of the salamander, *Necturus maculosus*. *Chem. Senses*, **27**, 673–680.

Fiala, A., Spall, T., Diegelmann, S., Eisermann, B., Sachse, S., Devaud, J.M., Buchner, E. & Galizia, C.G. (2002) Genetically expressed cameleon in *Drosophila melanogaster* is used to visualize olfactory information in projection neurons. *Curr. Biol.*, **12**, 1877–1884.

Fierro, L., DiPolo, R. & Llano, I. (1998) Intracellular calcium clearance in Purkinje cell somata from rat cerebellar slices. *J. Physiol.*, **510**, 499–512.

Ganeshina, O. & Menzel, R. (2001) GABA-immunoreactive neurons in the mushroom bodies of the honeybee: an electron microscopic study. *J. Comp. Neurol.*, **437**, 335–349.

Gomez, G., Lischka, F.W., Haskins, M.E. & Rawson, N.E. (2005) Evidence for multiple calcium response mechanisms in mammalian olfactory receptor neurons. *Chem. Senses*, **30**, 317–326.

Grunewald, B. (1999) Morphology of feedback neurons in the mushroom body of the honeybee, *Apis mellifera*. *J. Comp. Neurol.*, **404**, 114–126.

Guerini, D., Coletto, L. & Carafoli, E. (2005) Exporting calcium from cells. *Cell Calcium*, **38**, 281–289.

Guo, A.K., Liu, L., Xia, S.Z., Feng, C.H., Wolf, R. & Heisenberg, M. (1996) Conditioned visual flight orientation in *Drosophila*: dependence on age, practice and diet. *Learn. Mem.*, **3**, 49–59.

Haug-Collet, K., Pearson, B., Webel, R., Szerencsei, R.T., Winkfein, R.J., Schnetkamp, P.P.M. & Colley, N.J. (1999) Cloning and characterization of a potassium-dependent sodium/calcium exchanger in *Drosophila*. *J. Cell Biol.*, **147**, 659–669.

Heisenberg, M. (1998) What do the mushroom bodies do for the insect brain? An introduction. *Learn. Mem.*, **5**, 1–10.

Heisenberg, M. (2003) Mushroom body memoir: from maps to models. *Nat. Rev. Neurosci.*, **4**, 266–275.

Heisenberg, M., Borst, A., Wagner, S. & Byers, D. (1985) *Drosophila* mushroom body mutants are deficient in olfactory learning. *J. Neurogenet.*, **2**, 1–30.

Isaac, M.R., Elias, C.L., Le, H.D., Omelchenko, A., Hnatowich, M. & Hryshko, L.V. (2002) Inhibition of the *Drosophila* Na^+/Ca^{2+} exchanger, CALX1.1, by KB-R7943. *Ann. NY Acad. Sci.*, **976**, 543–545.

Iwamoto, T., Kita, S., Uehara, A., Inoue, Y., Taniguchi, Y., Imanaga, I. & Shigekawa, M. (2001) Structural domains influencing sensitivity to isothiourea derivative inhibitor KB-R7943 in cardiac Na^+/Ca^{2+} exchanger. *Mol. Pharmacol.*, **59**, 524–531.

Iwamoto, T., Watano, T. & Shigekawa, M. (1996) A novel isothiourea derivative selectively inhibits the reverse mode of Na^+/Ca^{2+} exchange in cells expressing NCX1. *J. Biol. Chem.*, **271**, 22391–22397.

Jeon, D., Yang, Y.M., Jeong, M.J., Philipson, K.D., Rhim, H. & Shin, H.S. (2003) Enhanced learning and memory in mice lacking Na^+/Ca^{2+} exchanger 2. *Neuron*, **38**, 965–976.

Joerges, J., Kuttner, A., Galizia, C.G. & Menzel, R. (1997) Representations of odour mixtures visualized in the honeybee brain. *Nature*, **387**, 285–288.

Kim, M.H., Lee, S.H., Park, K.H., Ho, W.K. & Lee, S.H. (2003) Distribution of K^+-dependent Na^+/Ca^{2+} exchangers in the rat supraoptic magnocellular neuron is polarized to axon terminals. *J. Neurosci.*, **23**, 11673–11680.

Lee, T., Lee, A. & Luo, L.Q. (1999) Development of the *Drosophila* mushroom bodies: sequential generation of three distinct types of neurons from a neuroblast. *Development.*, **126**, 4065–4076.

Liu, L., Wolf, R., Ernst, R. & Heisenberg, M. (1999) Context generalization in *Drosophila* visual learning requires the mushroom bodies. *Nature*, **400**, 753–756.

Miyawaki, A., Llopis, J., Heim, R., McCaffery, J.M., Adams, J.A., Ikura, M. & Tsien, R.Y. (1997) Fluorescent indicators for Ca^{2+} based on green fluorescent proteins and calmodulin. *Nature*, **388**, 882–887.

Miywaki, A., Griesbeck, O., Heim, R. & Tsien, R.Y. (1999) Dynamic and quantitative Ca^{2+} measurements using improved cameleons. *Proc. Natl Acad. Sci. USA*, **96**, 2135–2140.

Moore, C.L. (1971) Specific inhibition of mitochondrial Ca^{2+} transport by ruthenium red. *Biochem. Biophys. Res. Commun.*, **42**, 298–305.

Nakai, J., Ohkura, M. & Imoto, K. (2001) A high signal-to-noise Ca^{2+} probe composed of a single green fluorescent protein. *Nat. Biotechnol.*, **19**, 137–141.

Park, Y.B., Herrington, J., Babcock, D.F. & Hille, B. (1996) Ca^{2+} clearance mechanisms in isolated rat adrenal chromaffin cells. *J. Physiol.*, **492**, 329–346.

Philipson, K.D. & Nicoll, D.A. (2000) Sodium-calcium exchange: a molecular perspective. *Annu. Rev. Physiol.*, **62**, 111–133.

Rawson, N.E., Gomez, G., Cowart, B., Brand, J.G., Lowry, L.D., Pribitkin, E.A. & Restrepo, D. (1997) Selectivity and response characteristics of human olfactory neurons. *J. Neurophysiol.*, **77**, 1606–1613.

Reed, K.C. & Bygrave, F.L. (1974) The inhibition of mitochondrial calcium transport by lanthanides and ruthenium red. *Biochem. J.*, **140**, 143–155.

Reiff, D.F., Ihring, A., Guerrero, G., Isacoff, E.Y., Joesch, M., Nakai, J. & Borst, A. (2005) In vivo performance of genetically encoded indicators of neural activity in flies. *J. Neurosci.*, **25**, 4766–4778.

Restrepo, D. & Boyle, A.G. (1991) Stimulation of olfactory receptors alters regulation of [Cai] in olfactory neurons of the catfish (*Ictalurus punctatus*). *J. Membr. Biol.*, **120**, 223–232.

Ruknudin, A., Valdivia, C., Kofuji, P., Lederer, W.J. & Schulze, D.H. (1997) Na^+/Ca^{2+} exchanger in *Drosophila*: cloning, expression, and transport differences. *Am. J. Physiol.*, **273**, C257–C265.

Saris, N.E. & Carafoli, E.A. (2005) Historical review of cellular calcium handling, with emphasis on mitochondria. *Biochemistry (Mosc).*, **70**, 187–194.

Schwarz, E.M. & Benzer, S. (1997) Calx, a Na-Ca exchanger gene of *Drosophila* melanogaster. *Proc. Natl Acad. Sci. USA*, **94**, 10249–10254.

Strausfeld, N.J., Hansen, L., Li, Y.S., Gomez, R.S. & Ito, K. (1998) Evolution, discovery, and interpretations of arthropod mushroom bodies. *Learn. Mem.*, **5**, 11–37.

Tang, S.M. & Guo, A.K. (2001) Choice behavior of *Drosophila* facing contradictory visual cues. *Science*, **294**, 1543–1547.

Wachowiak, M., Denk, W. & Friedrich, R.W. (2004) Functional organization of sensory input to the olfactory bulb glomerulus analyzed by two-photon calcium imaging. *Proc. Natl Acad. Sci. USA*, **101**, 9097–9102.

Wanaverbecq, N., Marsh, S.J., Al-Qatari, M. & Brown, D.A. (2003) The plasma membrane calcium-ATPase as a major mechanism for intracellular

calcium regulation in neurones from the rat superior cervical ganglion. *J. Physiol.*, **550**, 83–101.

Wang, Y., Guo, H.F., Pologruto, T.A., Hannan, F., Hakker, I., Svoboda, K. & Zhong, Y. (2004) Stereotyped odor-evoked activity in the mushroom body of *Drosophila* revealed by green fluorescent protein-based Ca^{2+} imaging. *J. Neurosci.*, **24**, 6507–6514.

Wang, J.W., Wong, A.M., Flores, J., Vosshall, L.B. & Axel, R. (2003) Two-photon calcium imaging reveals an odor-evoked map of activity in the fly brain. *Cell.*, **112**, 271–282.

Wang, T., Xu, H., Oberwinkler, J., Gu, Y., Hardie, R.C. & Montell, C. (2005) Light activation, adaptation, and cell survival functions of the Na^{+}/Ca^{2+} exchanger CalX. *Neuron*, **45**, 367–378.

Watano, T., Kimura, J., Morita, T. & Nakanishi, H. (1996) A novel antagonist, 7943, of the Na^{+}/Ca^{2+} exchange current in guinea-pig cardiac ventricular cells. *Br. J. Pharmacol.*, **119**, 555–563.

Wilson, R.I. & Laurent, G. (2005) Role of GABAergic inhibition in shaping odor-evoked spatiotemporal patterns in the *Drosophila* antennal lobe. *J. Neurosci.*, **25**, 9069–9079.

Winkfein, R.J., Pearson, B., Ward, R., Szerencsei, R.T., Colley, N.J. & Schnetkamp, P.P. (2004) Molecular characterization, functional expression and tissue distribution of a second NCKX Na^{+}/Ca^{2+}–K^{+} exchanger from *Drosophila*. *Cell Calcium*, **36**, 147–155.

Yasuyama, K., Meinertzhagen, I.A. & Schurmann, F.W. (2002) Synaptic organization of the mushroom body calyx in *Drosophila* melanogaster. *J. Comp. Neurol.*, **445**, 211–226.

Yu, D., Baird, G.S., Tsien, R.Y. & Davis, R.L. (2003) Detection of calcium transients in *Drosophila* mushroom body neurons with camgaroo reporters. *J. Neurosci.*, **23**, 64–72.

Zars, T. (2000) Behavioral functions of the insect mushroom bodies. *Curr. Opin. Neurobiol.*, **10**, 790–795.